Available online at www.sciencedirect.com

ScienceDirect

Ceramics International 40 (2014) 4219–4224

CERAMICS INTERNATIONAL

www.elsevier.com/locate/ceramint

Electrochemical properties of $LiNiO_2$ cathode after TiO_2 or ZnO addition

Myoung Youp Song[a], Hun Uk Kim[a], Hye Ryoung Park[b,*]

[a]*Division of Advanced Materials Engineering, Research Center of Advanced Materials Development, Engineering Research Institute, Chonbuk National University, 567 Baekje-daero Deokjin-gu Jeonju, 561-756, Republic of Korea*

[b]*School of Applied Chemical Engineering, Chonnam National University, 77 Yongbong-ro Buk-gu Gwangju, 500-757, Republic of Korea*

Received 21 July 2013; received in revised form 8 August 2013; accepted 20 August 2013
Available online 7 September 2013

Abstract

$LiNiO_2$ was prepared by solid state reaction, and $LiNiO_2$ was mixed with 1-, 2-, or 5 wt% TiO_2 or ZnO for the preparation of cathodes for a lithium ion battery. The electrochemical properties of the cathodes were investigated and the effects of the addition of TiO_2 or ZnO were discussed. The voltage vs. capacity curves for charge and discharge at different numbers of cycles for $LiNiO_2$, 2 wt% TiO_2-added $LiNiO_2$, and 2 wt% ZnO_2-added $LiNiO_2$ showed that in all the samples the first discharge capacity is much smaller than the first charge capacity. The addition of TiO_2 or ZnO decreased the discharge capacities, but improved the cycling performance. The discharge capacities of $LiNiO_2$ and 2 wt% TiO_2-added $LiNiO_2$ decreased as the number of cycles increased. However, the discharge capacity of 2 wt% ZnO-added $LiNiO_2$ increased overall as the number of cycles increased. The $-dx/|dV|$ vs. voltage curves for the 1st and 2nd cycles of 0, 1-, 2-, or 5 wt% TiO_2 or ZnO-added $LiNiO_2$ showed that all the samples underwent four phase transitions during charging and discharging.

Keywords: $LiNiO_2$; Oxide addition; Electrochemical properties; First charge capacity; Discharge capacity

1. Introduction

Lithium transition metal oxides such as $LiCoO_2$ [1,2], $LiNiO_2$ [3,4], and $LiMn_2O_4$ [5,6] have been investigated as cathode electrode materials for rechargeable lithium batteries. $LiCoO_2$ has been studied most intensively for the application to commercial rechargeable batteries because of its large diffusivity and high operating voltage. However, it has drawbacks that cobalt is expensive and toxic. $LiMn_2O_4$ has several advantages that Mn is less expensive than other elements and its synthesis is easy, but its cycling performance is poor. $LiNiO_2$ is considered a promising cathode material due to its large discharge capacity and low cost. However, due to the size similarity of Li and Ni (Li^+=0.72 Å and Ni^{2+}=0.69 Å), $LiNiO_2$ is practically obtained in the non-stoichiometric composition $Li_{1-y}Ni_{1+y}O_2$ [7,8] and the Ni^{2+} ions in the lithium planes obstruct movement of Li^+ ions during charge and discharge [9,10].

In order to increase the discharge capacity and improve the cycling performance and structural stability of cathode materials, various elements were substituted for the transition elements in the cathode materials, and the surfaces of cathode materials were modified. Choblet et al. [11] showed that 2 wt% TiO_2-added $LiCoO_2$ had the best cycling performance and that the phase transition voltage for discharge changed. Researches on the surface modification, in which Co_3O_4 [12], Al_2O_3 [13,14], B_2O_3 [15], MgO [16,17], TiO_2 [15] or ZrO_2 [15] was added to $LiCoO_2$, have been presented. Oh et al. [13] reported that Al_2O_3 coating increases both the surface area and the electrical conductivity of $LiCoO_2$, improves the cycle performance even at a higher cut-off charge voltage, and induces higher thermal stability. Kweon et al. [16] reported that $Li_xNi_{1-y}Co_yO_2$, of which the surface is modified by coating $Mg(OH)_2$ and further heating the coated sample, had a lowered initial discharge capacity but had an improved cycle-reversibility. Wang et al. [17] studied commercial $LiCoO_2$ surfaces modified with MgO for lithium-ion batteries, and reported that surface modification can improve the structural stability of $LiCoO_2$ without decreasing its available specific

*Corresponding author. Tel.: +82 62 530 1885; fax: +82 62 530 1889.
E-mail address: hyrpark@naver.com (H.R. Park).

0272-8842/$ - see front matter © 2013 Elsevier Ltd and Techna Group S.r.l. All rights reserved.
http://dx.doi.org/10.1016/j.ceramint.2013.08.084

capacity. They attributed this improvement to the pillaring effect of the Mg^{2+} ions in the interslab space of the lattice and the protective effect of the MgO film against the escape of Co^{4+} ions from the bulk of the $LiCoO_2$ particles. Lu et al. [18] studied the anomalous capacity of $Li/Li[Ni_xLi_{(1/3-2x/3)}Mn_{(2/3-x/3)}]O_2$ cells using *in situ* X-ray diffraction, and reported that irreversible loss of oxygen from the compounds with $x < 1/2$ occurred during the first charge to 4.8 V, forming oxygen deficient layered materials, which reacted reversibly with lithium.

However, the surface modification of $LiNiO_2$ or the addition of oxides to $LiNiO_2$ was not reported. In this work, TiO_2 or ZnO was added to $LiNiO_2$ prepared by solid state reaction, and the electrochemical characteristics of the TiO_2 or ZnO-added cathode were investigated.

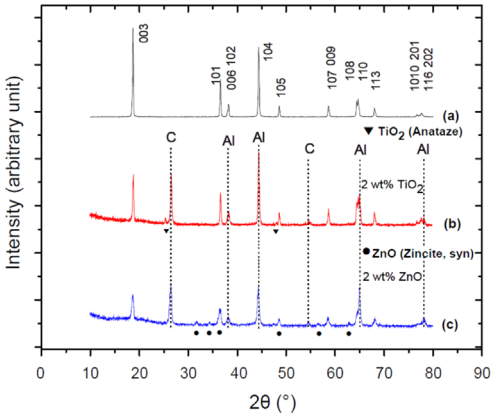

Fig. 1. XRD patterns of (a) $LiNiO_2$, (b) 2 wt% TiO_2-added $LiNiO_2$ after 5 cycles, and (c) 2 wt% ZnO-added $LiNiO_2$ after 5 cycles.

2. Experimental

$LiNiO_2$ was synthesized using a solid-state reaction method. $LiOH \cdot H_2O$ (Kojundo Chemical Lab. Co., Ltd, purity 99%) and $Ni(OH)_2$ (Kojundo Chemical Lab. Co., Ltd, purity 99.9%) were used as starting materials. The starting materials with a composition of $LiNiO_2$ were mixed mechanically with a SPEX mill for 1 h. The mixed material was preheated at 450 °C for 5 h in air, pressed into a pellet and then calcined at 750 °C for 30 h under oxygen stream. The $LiNiO_2$ sample, which was prepared under these conditions, showed the best electrochemical properties [19].

TiO_2 (anatase) (Aldrich Co., purity 99%) and ZnO (Aldrich Co., purity 99%) were used for 1, 2, or 5 wt% additions. TiO_2 or ZnO was mixed with $LiNiO_2$ for 24 h in a magnetic stirrer.

The samples were characterized by X-ray diffraction analysis (Rigaku III/A diffractometer) using Cu Kα radiation. The scanning rate was $6^\circ\,min^{-1}$ and the scanning range of diffraction angle (2θ) was $10^\circ \le 2\theta \le 80^\circ$.

The electrochemical cells consisted of $LiNiO_2$ or TiO_2 or ZnO-added $LiNiO_2$ as a cathode, Li foil as a anode, and electrolyte (Purelyte (Samsung General Chemicals Co., Ltd.)) prepared by solving 1 M $LiPF_6$ in an 1:1 (volume ratio) mixture of ethylene carbonate (EC) and diethyl carbonate (DEC). The cathode consisted of 85 wt% synthesized materials, 10 wt% acetylene black, and 5 wt% polyvinylidene fluoride (PVDF) binder solved in N-Methyl-2-pyrrolidinone (NMP), which were pasted on Al foil and dried at 353 K for 24 h. A Whatman glass-filer was used as a separator. The cells were assembled in an argon-filled dry box and the coin-type (2016) cell was employed. All the electrochemical tests were galvanostatically cycled in the voltage range 2.7–4.2 V at 0.1 C-rate.

3. Results and discussion

Fig. 1 shows the XRD patterns of $LiNiO_2$, 2 wt% TiO_2-added $LiNiO_2$ after 5 charge–discharge cycles, and 2 wt% ZnO-added $LiNiO_2$ after 5 charge–discharge cycles. All the samples exhibit peaks of the $LiNiO_2$ phase, which has a α-$NaFeO_2$ structure with a space group of $R\bar{3}m$. The XRD patterns of 2 wt% TiO_2-added $LiNiO_2$ after 5 charge–discharge cycles and 2 wt% ZnO-added $LiNiO_2$ after 5 charge–discharge cycles show C peaks from acetylene black at the diffraction angles of 26.4° and 54.5°, Al peaks from aluminum foil at the diffraction angles of 38.5°, 44.7°, 65.1°, and 78.2°, and TiO_2 or ZnO peaks.

The SEM micrographs of $LiNiO_2$, 2 wt% TiO_2-added $LiNiO_2$, and 2 wt% TiO_2-added $LiNiO_2$ after 5 cycles are shown in Fig. 2. The particles of $LiNiO_2$ in the $LiNiO_2$ sample are polyhedral while those in the samples of 2 wt% TiO_2-added $LiNiO_2$ and 2 wt% TiO_2-added $LiNiO_2$ after 5 cycles are large and thin. TiO_2 exists in the form of fine particles. The 2 wt% TiO_2-added $LiNiO_2$ before charge–discharge cycling and 2 wt% TiO_2-added $LiNiO_2$ after 5 cycles have similar microstructures.

Fig. 3 shows the SEM micrographs of 2 wt% ZnO_2-added $LiNiO_2$ and 2 wt% ZnO_2-added $LiNiO_2$ after 5 cycles. The microstructures of these two samples are very similar. No large difference is observed between the microstructures of these two samples and those of the 2 wt% TiO_2-added $LiNiO_2$ before charge–discharge cycling and the 2 wt% TiO_2-added $LiNiO_2$ after 5 cycles.

The voltage vs. capacity curves for charge and discharge at different numbers of cycles for $LiNiO_2$, 2 wt% TiO_2-added $LiNiO_2$, and 2 wt% ZnO_2-added $LiNiO_2$ are shown in Fig. 4. All the samples showed much smaller charge capacity at the second cycle than at the first cycle, and the charge capacities at the 5th cycle are slightly smaller than those at the second cycle. In all the samples, the first discharge capacity is much smaller than the first charge capacity. It is believed that this is because at the first charging, the Li ions that entered the Ni sites deintercalate.

Fig. 5 shows the variations of discharge capacity at 0.1 C-rate with the number of cycles for $LiNiO_2$, 2 wt% TiO_2-added $LiNiO_2$, and 2 wt% ZnO-added $LiNiO_2$. $LiNiO_2$ has the largest first discharge capacity of 164.7 mA h/g, followed in order by 2 wt% TiO_2-added $LiNiO_2$ (135.8 mA h/g) and 2 wt% ZnO-added $LiNiO_2$ (112.5 mA h/g). The TiO_2 or ZnO-added $LiNiO_2$ sample has smaller discharge capacities than the $LiNiO_2$

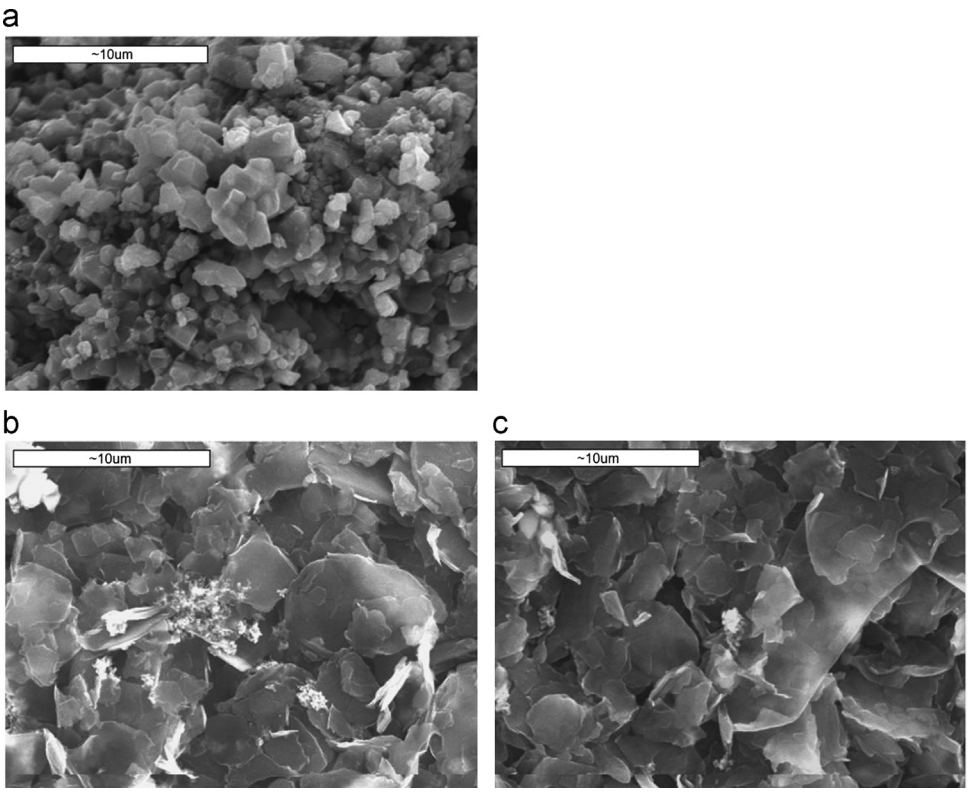

Fig. 2. SEM micrographs of (a) $LiNiO_2$, (b) 2 wt% TiO_2-added $LiNiO_2$, and (c) 2 wt% TiO_2-added $LiNiO_2$ after 5 cycles.

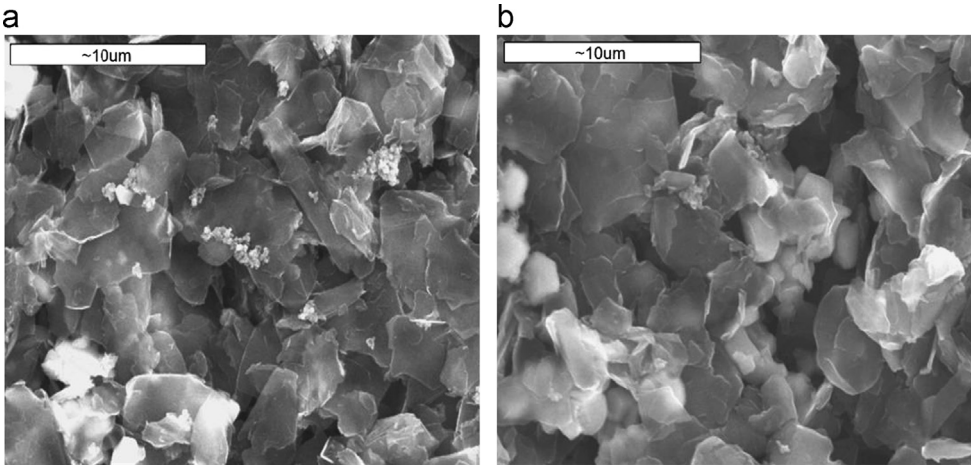

Fig. 3. SEM micrographs of (a) 2 wt% ZnO_2-added $LiNiO_2$, and (b) 2 wt% ZnO_2-added $LiNiO_2$ after 5 cycles.

sample. It is believed that this is because the addition of TiO_2 or ZnO decreases the fraction of the $LiNiO_2$ phase and the area of reaction interface. The addition of TiO_2 or ZnO decreases the discharge capacities, but improves the cycling performance. The discharge capacities of $LiNiO_2$ and 2 wt% TiO_2-added $LiNiO_2$ decrease as the number of cycles increases. However, the discharge capacity of 2 wt% ZnO-added $LiNiO_2$ increases overall as the number of cycles increases probably because the area of reaction interface increases due to the separation of ZnO from $LiNiO_2$ with the increase in the number of cycles.

The variations of the first discharge capacity and the capacity deterioration rate of $LiNiO_2$, 2 wt% TiO_2-added $LiNiO_2$, and 2 wt% ZnO-added $LiNiO_2$ are shown in Fig. 6. $LiNiO_2$ has the largest capacity deterioration rate of 4.35 mA h/g/cycle, followed in order by 2 wt% TiO_2-added $LiNiO_2$ (1.01 mA h/g/cycle) and 2 wt% ZnO-added $LiNiO_2$ (-1.25 mA h/g/cycle). The discharge capacity of 2 wt% ZnO-added $LiNiO_2$ increases as the number of cycles increases. The sample with a large first discharge capacity exhibits a large capacity deterioration rate. A larger first discharge capacity corresponds to a larger amount of intercalation of Li, which is related to the wider change of the

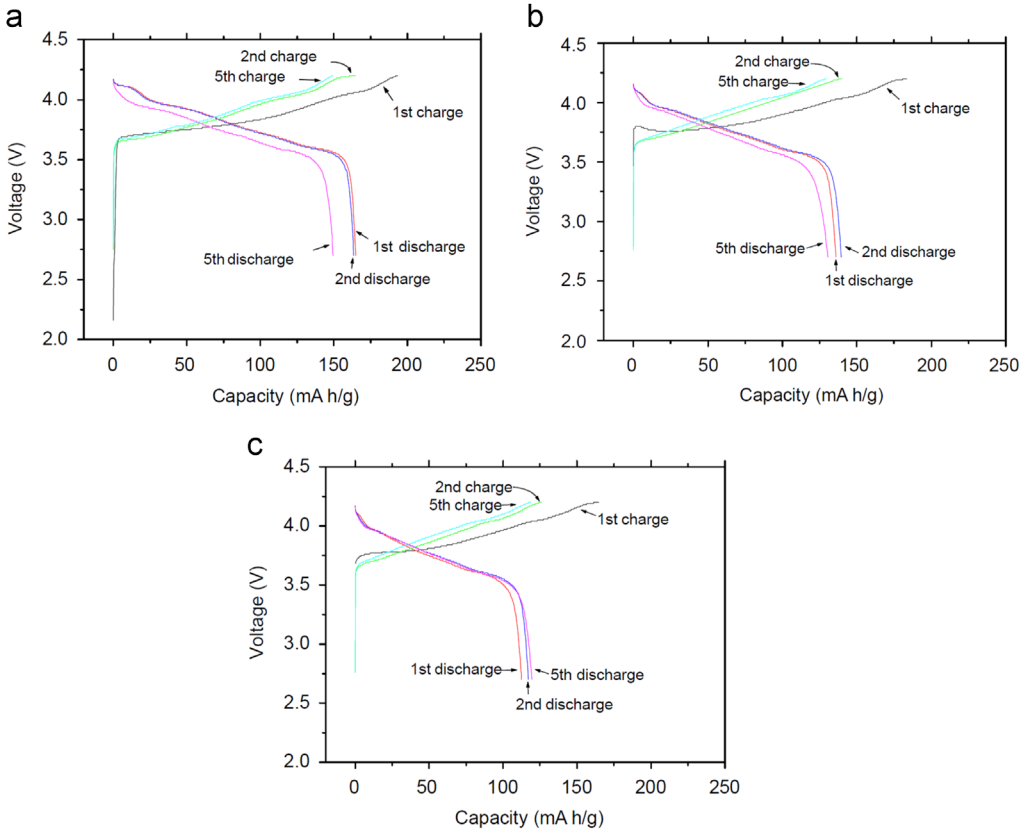

Fig. 4. Charge–discharge curves for the various numbers of cycles for (a) $LiNiO_2$, (b) 2 wt%TiO_2-added $LiNiO_2$, and (c) 2 wt% ZnO_2-added $LiNiO_2$.

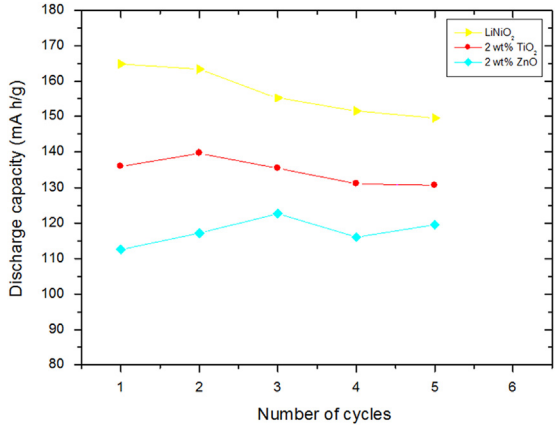

Fig. 5. Variations of discharge capacity at 0.1 C-rate with the number of cycles for $LiNiO_2$, 2 wt% TiO_2-added $LiNiO_2$, and 2 wt% ZnO-added $LiNiO_2$.

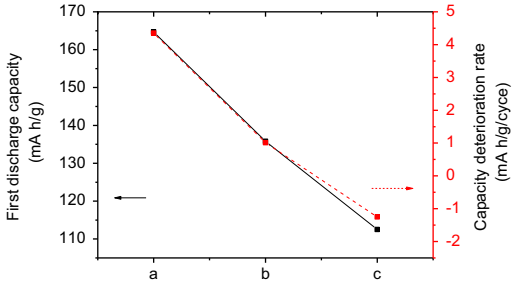

Fig. 6. Variations of the first discharge capacity and the capacity deterioration rate of (a) $LiNiO_2$, (b) 2 wt% TiO_2-added $LiNiO_2$, and (c) 2 wt% ZnO-added $LiNiO_2$.

value of x in Li_xNiO_2. The larger change of the value of x will cause larger expansion and contraction of the $LiNiO_2$ phase with the α-$NaFeO_2$ structure due to the intercalation and deintercalation. This will make the unit cell strained and distorted. With cycling, the interstitial sites and thus the α-$NaFeO_2$ structure will be destroyed. This decreases the fraction of the $LiNiO_2$ phase, leading to the capacity fading of $LiNiO_2$ with cycling. For the samples with smaller discharge capacity, the expansion and contraction due to intercalation and deintercalation can be within the limit of elasticity of $LiNiO_2$, and the lattice destruction can thus be small. The discharge capacity can accordingly decrease slowly with cycling (i.e., the capacity fading rate can be low).

Fig. 7 shows $-dx/|dV|$ vs. voltage curves for the 1st and 2nd cycles of $LiNiO_2$, 1 wt% TiO_2-added $LiNiO_2$, 2 wt% TiO_2-added $LiNiO_2$, and 5 wt% TiO_2-added $LiNiO_2$. At the peaks of the $-dx/|dV|$ vs. voltage curves, two phases co-exist. All the samples undergo four phase transitions during charging: from a hexagonal structure (H1) to a monoclinic structure (M), from the monoclinic structure (M) to a hexagonal structure (H2), from the hexagonal structure (H2) to hexagonal structures (H2+H3), and from the hexagonal structures (H2+H3) to a hexagonal structure (H3). All the samples also undergo four phase transitions during discharging: from the hexagonal structure (H3) to the hexagonal structures (H2+H3), from

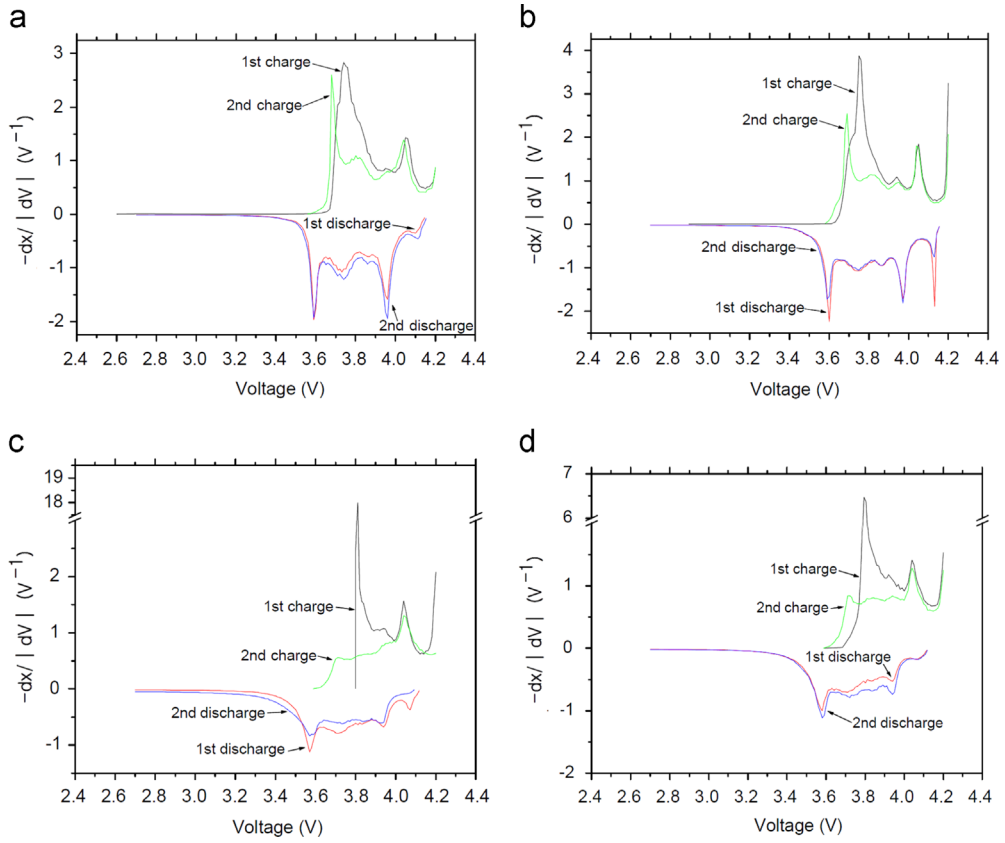

Fig. 7. −d*x*/d*V* vs. voltage curves for the 1st and 2nd cycles of (a) $LiNiO_2$, (b) 1 wt% TiO_2-added $LiNiO_2$, (c) 2 wt% TiO_2-added $LiNiO_2$, and (d) 5 wt% TiO_2-added $LiNiO_2$.

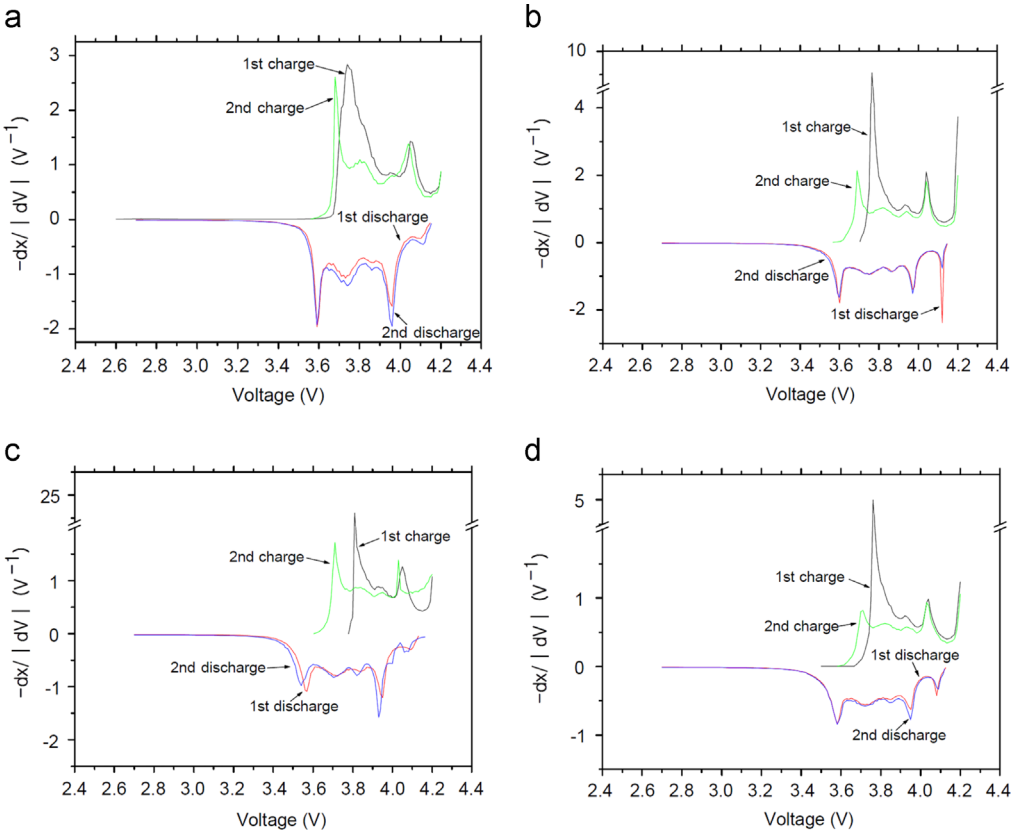

Fig. 8. −d*x*/d*V* vs. voltage curves for the 1st and 2nd cycles of (a) $LiNiO_2$, (b) 1 wt% ZnO_2-added $LiNiO_2$, (c) 2 wt% ZnO_2-added $LiNiO_2$, and (d) 5 wt% ZnO_2-added $LiNiO_2$.

the hexagonal structures (H2 + H3) to the hexagonal structure (H2), from the hexagonal structure (H2) to the monoclinic structure (M), and from the monoclinic structure (M) to the hexagonal structure (H1). For 2 wt% TiO_2-added $LiNiO_2$ and 5 wt% TiO_2-added $LiNiO_2$, at the first charging the peak for the phase transition from the hexagonal structure (H1) to the monoclinic structure (M) is very strong, but at the second charging it is weak. For discharging, the peaks become weaker as the added quantity of TiO_2 increases. The voltages of peaks for discharging are lower than those for charging.

The $-dx/|dV|$ vs. voltage curves for the 1st and 2nd cycles of $LiNiO_2$, 1 wt% ZnO_2-added $LiNiO_2$, 2 wt% ZnO_2-added $LiNiO_2$, and 5 wt% ZnO_2-added $LiNiO_2$ are shown in Fig. 8. ZnO_2-added $LiNiO_2$ samples show similar behaviors to TiO_2-added $LiNiO_2$ samples. For 1 wt% TiO_2-added $LiNiO_2$, 2 wt% TiO_2-added $LiNiO_2$, and 5 wt% TiO_2-added $LiNiO_2$, at the first charging the peak for the phase transition from the hexagonal structure (H1) to the monoclinic structure (M) is very strong, but at the second charging it is weak.

4. Conclusions

$LiNiO_2$ was prepared by solid state reaction, and $LiNiO_2$ was mixed with 1-, 2-, or 5 wt% TiO_2 or ZnO for the preparation of cathodes. The voltage vs. capacity curves for charge and discharge at different numbers of cycles for $LiNiO_2$, 2 wt% TiO_2-added $LiNiO_2$, and 2 wt% ZnO_2-added $LiNiO_2$ showed that in all the samples the first discharge capacity is much smaller than the first charge capacity probably because at the first charging Li ions which entered the Ni sites deintercalate. The addition of TiO_2 or ZnO decreased the discharge capacities, but improved the cycling performance. The discharge capacities of $LiNiO_2$ and 2 wt% TiO_2-added $LiNiO_2$ decreased as the number of cycles increased. However, the discharge capacity of 2 wt% ZnO-added $LiNiO_2$ increased overall as the number of cycles increased probably because the area of reaction interface increases due to the separation of ZnO from $LiNiO_2$ with the increase in the number of cycles. All the samples underwent four phase transitions during charging: from a hexagonal structure (H1) to a monoclinic structure (M), from the monoclinic structure (M) to a hexagonal structure (H2), from the hexagonal structure (H2) to hexagonal structures (H2 + H3), and from the hexagonal structures (H2 + H3) to a hexagonal structure (H3).

References

[1] K. Ozawa, Lithium-ion rechargeable batteries with $LiCoO_2$ and carbon electrodes: the $LiCoO_2$/C system, Solid State Ionics 69 (1994) 212–221.

[2] Z.S. Peng, C.R. Wan, C.Y. Jiang, Synthesis by sol–gel process and characterization of $LiCoO_2$ cathode materials, Journal of Power Sources 72 (1998) 215–220.

[3] J.R. Dahn, U. von Sacken, M.W. Juzkow, H. Al-Janaby, Rechargeable $LiNiO_2$/carbon cells, Journal of the Electrochemical Society 138 (1991) 2207–2212.

[4] M.Y. Song, R. Lee, Synthesis by sol–gel method and electrochemical properties of $LiNiO_2$ cathode material for lithium secondary battery, Journal of Power Sources 111 (1) (2002) 97–103.

[5] J.M. Tarascon, E. Wang, F.K. Shokoohi, W.R. Mckinnon, S. Colson, The spinel phase of $LiMn_2O_4$ as a cathode in secondary lithium cells, Journal of the Electrochemical Society 138 (1991) 2859–2864.

[6] M.Y. Song, D.S. Ahn, Improvement in the cycling performance of $LiMn_2O_4$ by the substitution of Fe for Mn, Solid State Ionics 112 (1998) 245–248.

[7] P. Barboux, J.M. Tarascon, F.K. Shokoohi, The use of acetates as precursors for the low-temperature synthesis of $LiMn_2O_4$ and $LiCoO_2$ intercalation compounds, Journal of Solid State Chemistry 94 (1991) 185–196.

[8] J. Morales, C. Perez-Vicente, J.L. Tirado, Cation distribution and chemical deintercalation of $Li_{1-x}Ni_{1+x}O_2$, Materials Research Bulletin 25 (1990) 623–630.

[9] A. Rougier, I. Saadoune, P. Gravereau, P. Willmann, C. Delmas, Effect of cobalt substitution on cationic distribution in $LiNi_{1-y}Co_yO_2$ electrode materials, Solid State Ionics 90 (1996) 83–90.

[10] B.J. Neudecker, R.A. Zuhr, B.S. Kwak, J.B. Bates, J.D. Robertson, Lithium manganese nickel oxides $Li_x(Mn_yNi_{1-y})_{2-x}O_2$, Journal of the Electrochemical Society 145 (1998) 4148–4157.

[11] A. Choblet, H.C. Shiao, H.P. Lin, M. Salomon, V. Manivannan, Two-phase $LiCoO_2$ oxides for rechargeable lithium batteries, Electrochemical and Solid-State Letters 4 (6) (2001) A65–A67.

[12] G.T.K. Fey, Y.Y. Lin, T. Prem Kumar, Enhanced cyclability and thermal stability of $LiCoO_2$ coated with cobalt oxides, Surface & Coatings Technology 191 (2005) 68–75.

[13] S.S. Oh, J.K. Lee, D.I. Byun, W.I. Cho, B.W. Cho, Effect of Al_2O_3 coating on electrochemical performance of $LiCoO_2$ as cathode materials for secondary lithium batteries, Journal of Power Sources 132 (2004) 249–255.

[14] J.P. Cho, Y.J. Kim, B.W. Park, $LiCoO_2$ cathode material that does not show a phase transition from hexagonal to monoclinic phase, Journal of the Electrochemical Society 148 (10) (2001) A1110–1115.

[15] J.P. Cho, Y.J. Kim, T.J. Kim, B.W. Park, Zero-strain intercalation cathode for rechargeable Li-ion cell, Angewandte Chemie International Edition 40 (18) (2001) 3367–3369.

[16] H.J. Kweon, S.J. Kim, D.G. Park, Modification of $Li_xNi_{1-y}Co_yO_2$ by applying a surface coating of MgO, Journal of Power Sources 88 (2000) 255–261.

[17] Z. Wang, C. Wu, L. Liu, F. Wu, L. Chen, X. Huang, Electrochemical evaluation and structural characterization of commercial $LiCoO_2$ surfaces modified with MgO for lithium-ion batteries, Journal of the Electrochemical Society 149 (4) (2002) A466–471.

[18] Z. Lu, J.R. Dahn, Understanding the anomalous capacity of Li/Li $[Ni_xLi_{(1/3-2x/3)}Mn_{(2/3-x/3)}]O_2$ cells using in situ X-ray diffraction and electrochemical studies, Journal of the Electrochemical Society 149 (2002) A815–822.

[19] H.U. Kim, S.D. Youn, J.C. Lee, H.R. Park, M.Y. Song, Study on the synthesis by milling and solid-state reaction method and electrochemical properties of $LiNiO_2$, Journal of Korean Ceramic Society 42 (5) (2005) 319–325.